Engineering Structures 207 (2020) 110223

Contents lists available at ScienceDirect

Engineering Structures

journal homepage: www.elsevier.com/locate/engstruct

Numerical study on seismic performance of prefabricated steel frames with recentering energy dissipative braces

Quanxi Ye[a,b,c], Zongyi Wang[a,b,*], Yuanqing Wang[b]

[a] School of Civil Engineering and Mechanics, Huazhong University of Science and Technology, Wuhan 430074, China
[b] Department of Civil Engineering, Tsinghua University, Beijing 100084, China
[c] Hebei University of Water Resources and Electric Engineering, Cangzhou 061001, China

ARTICLE INFO

Keywords:
Prefabricated structure
RCED brace
SCED brace
Hysteretic response
Time history analysis

ABSTRACT

The application and research of prefabricated steel structures (PPSs) have developed rapidly in China. To improve the seismic resistance of PPSs, alternative bracing systems have been developed. The seismic performance of steel frames with recentering energy dissipative (RCED) braces is investigated numerically through quasistatic and nonlinear time history analyses. A one-bay braced frame model was first created in ABAQUS and calibrated by previous experimental tests. Subsequently, a comparative study on the dynamic performances of the multistory steel frames with RCED braces and self-centering energy dissipative braces was conducted. Six far-field earthquake records were adopted, i.e., Northridge, Imperial Valley, Kobe, San Fernando, Loma Prieta, and Kocaeli, Turkey. Finally, a parametric study was performed to investigate the effects of tendon diameter and pretension magnitude of high-strength bolts on the seismic performances of the RCED model under the Kocaeli earthquake.

1. Introduction

Prefabricated steel structures (PSSs) are a new type of structure that embodies the definition of a green building [1,2]. PSS models are manufactured in factories and assembled with bolt connections on site [3]. Compared with traditional steel buildings and structures, PSSs can reduce more energy, shorten construction period, reduce contamination, and protect the environment in its life cycle.

A steel braced frame is a reliable structure that can resist earthquake. The traditional seismic design of structures is based on the anticollapse concept. The energy of an earthquake is dissipated by the plastic hinges formed in beam-to-column joints or the yielding of braces. When braces are buckled, the load-bearing and energy dissipation capacities of the braces are affected significantly. Hence, researchers worldwide have developed various types of buckling-restrained braces (BRBs) [4–6].

Traditional BRBs have successfully solved the buckling problem of braces, while steel frames with BRBs will experience large peak deformations and excessive interstory drifts in rare earthquake events. Some evidence has shown that the repairing cost will be higher than the reconstruction cost if the residual interstory drift is larger than 0.5% [7]. Additionally, the *P*-delta effect is significant in this type of structures and causes successive load cycles to pull the structure further in the same direction [8]. Based on the considerations above, self-centering systems have been developed by researchers. These types of systems can pull a structure back to its initial position after each load cycle, which can eliminate post-earthquake residual drifts. The following materials are frequently used for self-centering systems: post-tensioned (PT) tendons, shape memory alloys (SMAs), and springs.

Another importance aspect is the energy dissipative element. BRBs dissipate energy by their core steels, which may yield under repeated load actions. SMAs possess self-centering capacity and exhibit energy dissipation behaviors. However, SMAs have a worse energy dissipation capacity and a higher economic cost than mild structural steels [9]. Frictional devices are an alternative option for energy dissipation [10]. The hysteretic response of the friction-type self-centering energy dissipative (SCED) brace is shown in Fig. 1(a). Some studies [11,12] have shown that the peak interstory drifts of steel frames decrease and the system demonstrates better resistance against collapse under rare earthquake events if SCED braces are used.

As previously mentioned, SMAs and springs are adopted in self-centering systems. Because these materials are expensive or difficult to be installed, they cannot be easily scaled to all types of braced frames. Therefore, PT tendons are a promising option for self-centering systems. Both high-strength steel and composite polymer materials can be used for PT tendons. In general, high-strength steel has a lower economic

* Corresponding author at: School of Civil Engineering and Mechanics, Huazhong University of Science and Technology, Wuhan 430074, China.
E-mail address: wangzongyi1990@outlook.com (Z. Wang).

https://doi.org/10.1016/j.engstruct.2020.110223
Received 13 July 2019; Received in revised form 6 January 2020; Accepted 12 January 2020
Available online 28 January 2020

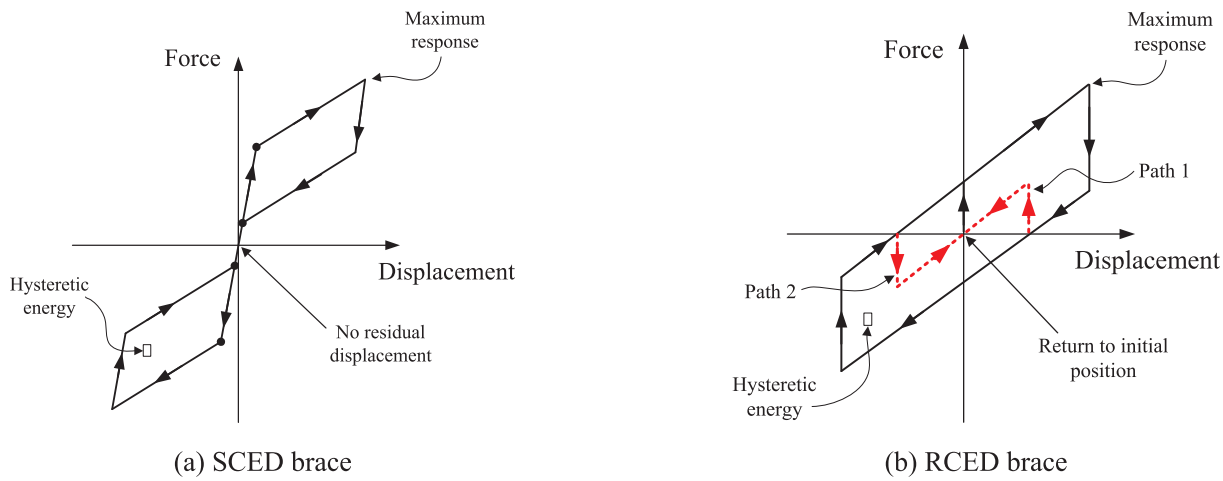

Fig. 1. Hysteretic responses of SCED and RCED braces.

cost and worse elongation capacity than composite polymer materials. A preload is always applied to the tendon to ensure that the brace can be pulled back to its original position. Some studies have shown that high-strength steel tendons do not perform well as expected due to the loss of initial PT force, especially when the preload is lower than 16% of the breaking force of the tendons [13,14]. Even though the effect of pretension loss is reduced when the preload reaches 30–40% of the breaking force, the increase in preloads on tendons will further decrease the elongation capacity of the tendons.

Hence, Zhang and Ye [15] developed an innovative recentering energy dissipative (RCED) brace. The hysteretic response of the RCED is depicted in Fig. 1(b) and its mechanics shown in Fig. 2. The RCED brace comprises a frictional energy dissipative device, an inner member, an outer member, two fixed ends, and two groups of steel tendons. Each group had four tendons without preload and only one group of tendons operated whether in tension or compression. The frictional energy dissipative device is shown in Fig. 3. Owing to friction, the inner member would not return to the zero deformation location after each load cycle; however, if the high-strength bolts in the fictional device were loosened after a vibration, the brace would still return to its initial location.

The aim of the present study is to investigate the seismic performance of steel frames with RCED braces by finite element analysis

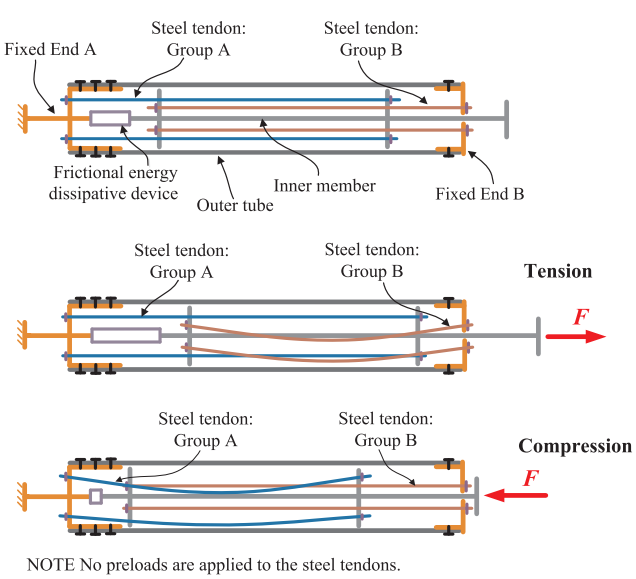

Fig. 2. RCED brace mechanics.

(FEA). This paper includes two parts: quasistatic analysis of nonmoment steel frame with an RCED brace and dynamic (time history) analysis of multistory building with RCED braces. It is noteworthy that the hysteretic behavior of the RCED braced frame has been studied experimentally in [15]. Therefore, the main goal of the quasistatic analysis is to verify the finite element (FE) model and the simplification method of the RCED brace; the hysteretic behavior of RCED braced frame is not discussed in detail in the present study.

2. Description of the experimental test on the RCED braced frame

Three prefabricated steel frames with RCED braces (RCED-BF-a, RCED-BF-b, and RCED-BF-c) were designed and tested under cyclic loads [15], as shown in Fig. 4. Each steel frame comprised two columns with a square hollow section (SHS), two brackets, and an I-beam. The dimensions of each member are depicted in Fig. 4. The description of the tendons and high-strength bolts used in the RCED braced frames is shown in Table 1. The Young's modulus of the columns, brackets, and I-beams was 206 GPa, the Poisson's ratio 0.3, and the yield strength 352 MPa. The Young's modulus of the steel tendons was 114 GPa and the Poisson's ratio 0.3.

Combinations of the columns and brackets were prefabricated in a factory and connected with the I-beam using bolts on site. The design of these prefabricated steel frames followed the principle that the braces dissipated almost all the energy, and plastic hinges were prohibited in the steel frames. Therefore, the prefabricated steel frames were designed to be nonmoment-resisting frames. Some studies on nonmoment-resisting frames have been reported [16,17], which are suitable for prefabricated buildings because bolt connections are advantageous for on-site installations.

A vertical load of 1000 kN, approximately equal to an axial compression ratio of 0.3, was applied to each column, and a cyclic load was applied at the top of a column. The maximum loading displacements of each loading step are listed in Table 2. It is worthy to note that the steel frames experienced two identical load cycles at each loading step. The hysteresis loops of the steel frames obtained from the tests were used for calibrating the FE model in the next section.

3. Quasistatic analysis of the tested RCED braced frames

In the FEA, it is unrealistic to model each part of the RCED brace, especially when modeling a multistory building with numerous RCED braces. Therefore, a simplified model of the RCED brace should be developed.

Numerical simulations of the experimental tests were performed using the ABAQUS software. The FE model is shown in Fig. 5. As the

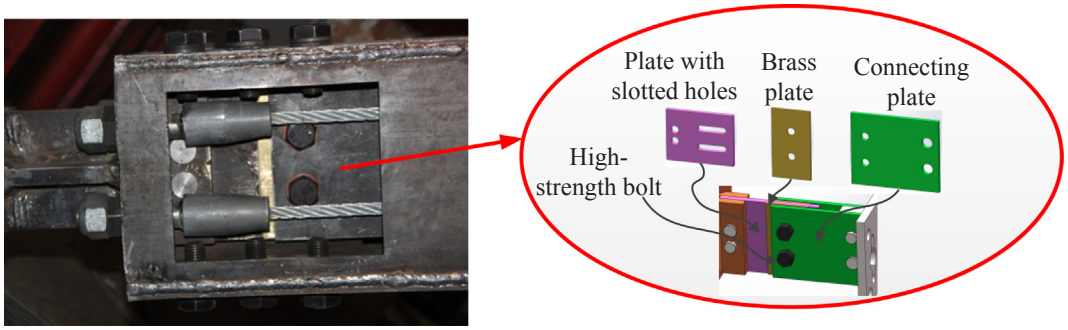

Fig. 3. Frictional energy dissipative device.

brackets were short and only used to connect the I-beam and columns, they were ignored in the FE models and the I-beam was directly connected to the columns with pin joints. B31 elements (two-node linear beam element) were employed for the columns and I-beams. The dimensions described in Fig. 4(a) were adopted for these members. The tendons in the RCED brace were simulated by a steel member that was modeled using T3D2 elements (two-node linear three-dimensional truss elements). The cross-sectional area of this member was four times the effective cross-sectional area of the tendon, and the length was equal to those of the tendons. The frictional device in the RCED brace was modeled using the *Axial*-type connector (which defines the friction behavior) in the *Interaction* section in ABAQUS, as shown in Fig. 5(a).

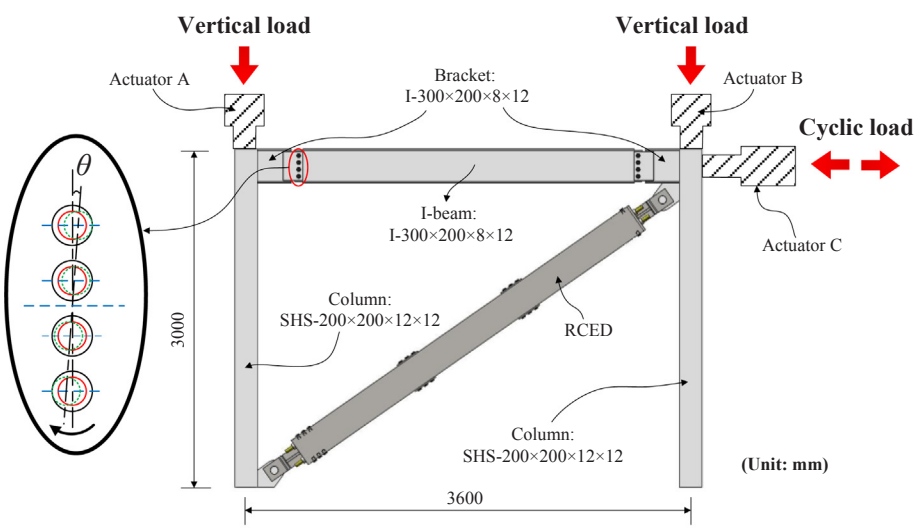

(a) schematic diagram

(b) photograph of experimental test

Fig. 4. Test on prefabricated steel frames with RCED brace.

Table 1
Description of tendons and high-strength bolts used for each braced frame in tests.

Type	Tendons					High-strength bolts		
	Diameter (mm)	Effective cross-sectional area (mm^2)	Length (mm)	Number (for each group)	Breaking force (kN)	Diameter (mm)	Pretension (kN)	Number
RCED-BF-a	17	107.8	3800	4	146.3	16	100	2
RCED-BF-b	17	107.8	3800	4	146.3	20	155	2
RCED-BF-c	21.5	186.6	3800	4	237.6	20	155	2

Table 2
Maximum horizontal displacement of RCED-BFs.

Loading step	1	2	3	4	5	6
Maximum displacement (mm)	10.0	20.0	30.0	40.0	50.0	60.0

The coefficient of friction was set to 0.26 [15], and the contact forces between Points A and C were four times (two brass plates and two high-strength bolts) the pretensions of the high-strength bolts. It is noteworthy that the outer tube, inner member, fixed ends, and free end of the RCED brace were employed to transfer loads and not modeled herein for simplicity. The connections between the I-beams and columns were simulated using the *Join + Rotation* type connector, which only restrained the translations of the nodes. Kinematic couplings were

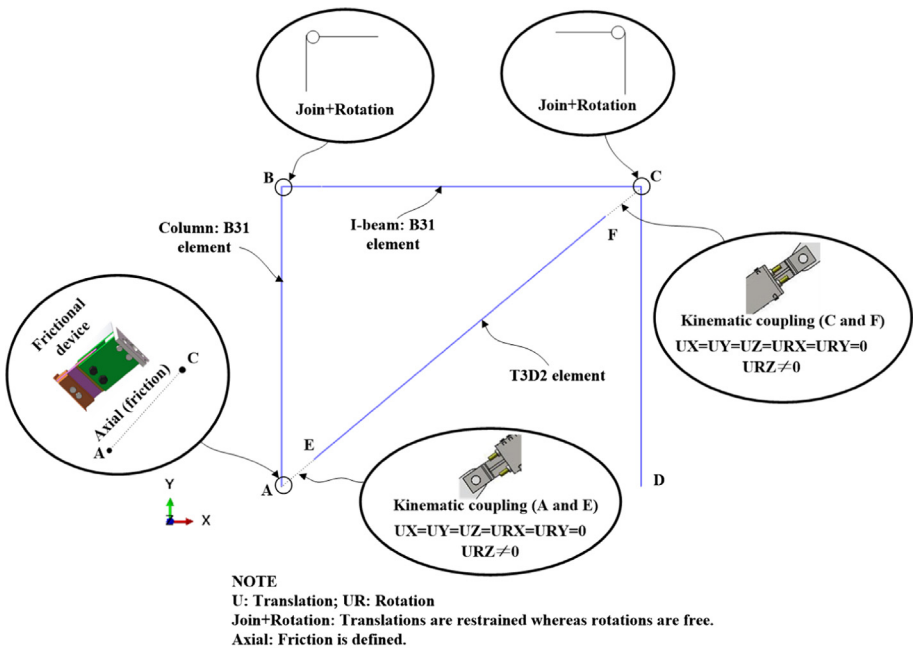

(a) element types and connections

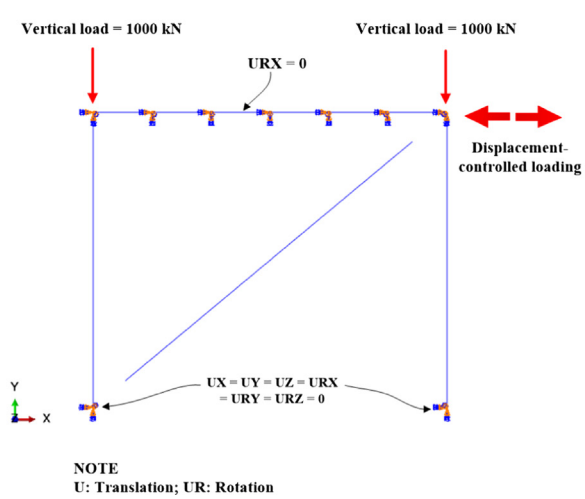

(b) loading scheme and boundary conditions

Fig. 5. FE model of single steel frame.

used to define the connections of the members (tendons) and steel frames.

Fig. 5(b) shows the boundary conditions and loading scheme of the FE models. To prevent the I-beam from rotating, an out-of-plane constraint was applied to the I-beam (see Fig. 4(b)). Therefore, rotation in the x axis direction was restrained for the I-beam, in accordance with reality. Furthermore, it is noteworthy that the rotations of the I-beams were not restrained in the later FE simulations of multistory buildings (Section 4), because the floors could restrain the I-beams. For the foundations of the RCED-BFs, all the degrees of freedom were restrained. Two analysis steps were defined in each FE model. In the first step, the vertical loads were applied to the columns. In the second step, a displacement-controlled loading in accordance with the tests was performed. The structure would experience large deformations in the loading process. Hence, the large deflection effect was considered in the FE models.

The tendons remained elastic in the tests; therefore an elastic model was used for the steel members. The Young's modulus of the steel tendons was 114 GPa and the Poisson's ratio 0.3. The test results suggested that the I-beams and brackets were in an elastic stage in the loading processes, while the bottoms of the columns yielded under large deformations [15]. To model the experimental tests more accurately, an elastic–plastic model was used for the columns and I-beams. The Young's modulus of Q345 was 206 GPa, Poisson's ratio 0.3, and yield strength 352 MPa. The plastic data of Q345 steel obtained from coupon tests, which are not discussed in detail herein, were employed as well.

The comparison between experimental and numerical hysteresis loops is presented in Fig. 6. The FE results coincide well with the test results, especially for RCED-BF-a. Small discrepancies were discovered between the FE and test results for RCED-BF-b and RCED-BF-c, which may be caused by the yielding of the steel frames (bottoms of the columns) in the FE models. Several coupon tests of Q345 steel were carried out, among which the smallest yield strength was 352 MPa. However, this value was used in this study for a conservative design. It appears that the yield strengths of the steels in RCED-BF-b and RCED-BF-c were larger than 352 MPa. It was evident that the external force was relatively small in RCED-BF-a FE model; therefore, the yielding of the steel frame was insignificant. Consequently, the FE results of RCED-BF-a were similar to the test results. The comparison analysis demonstrated that these FE models were sufficiently accurate for providing valid results, and the feasibility of this simplification method was verified.

The test curves indicated the prominent recentering capacity of the steel frame. Residual deformations of the tested frames were discovered after the entire loading process. However, the structures returned to their zero-deformation locations when the high-strength bolts were loosened, which was difficult to be modeled in the FEA.

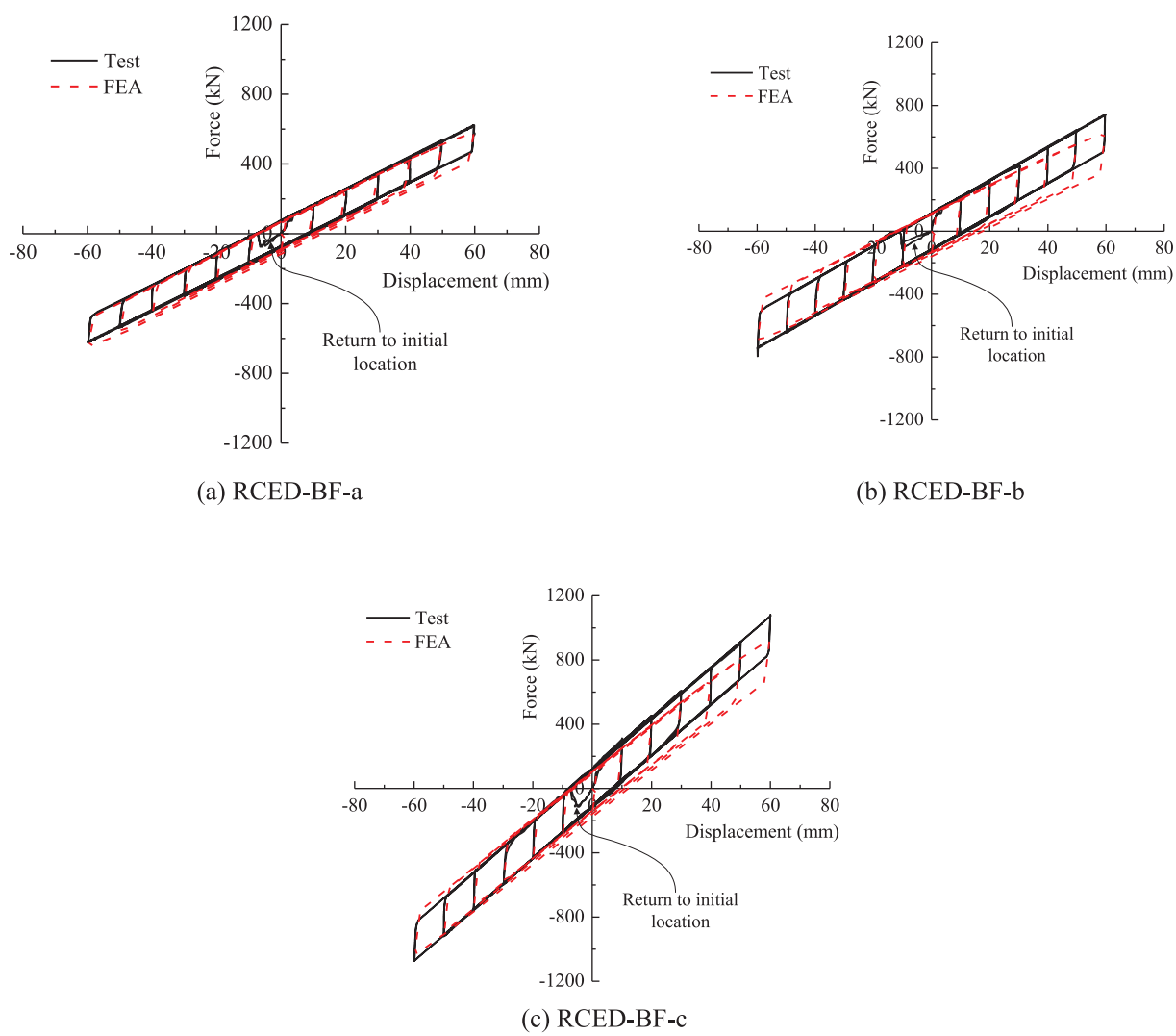

Fig. 6. Comparison between experimental and numerical hysteresis loops.

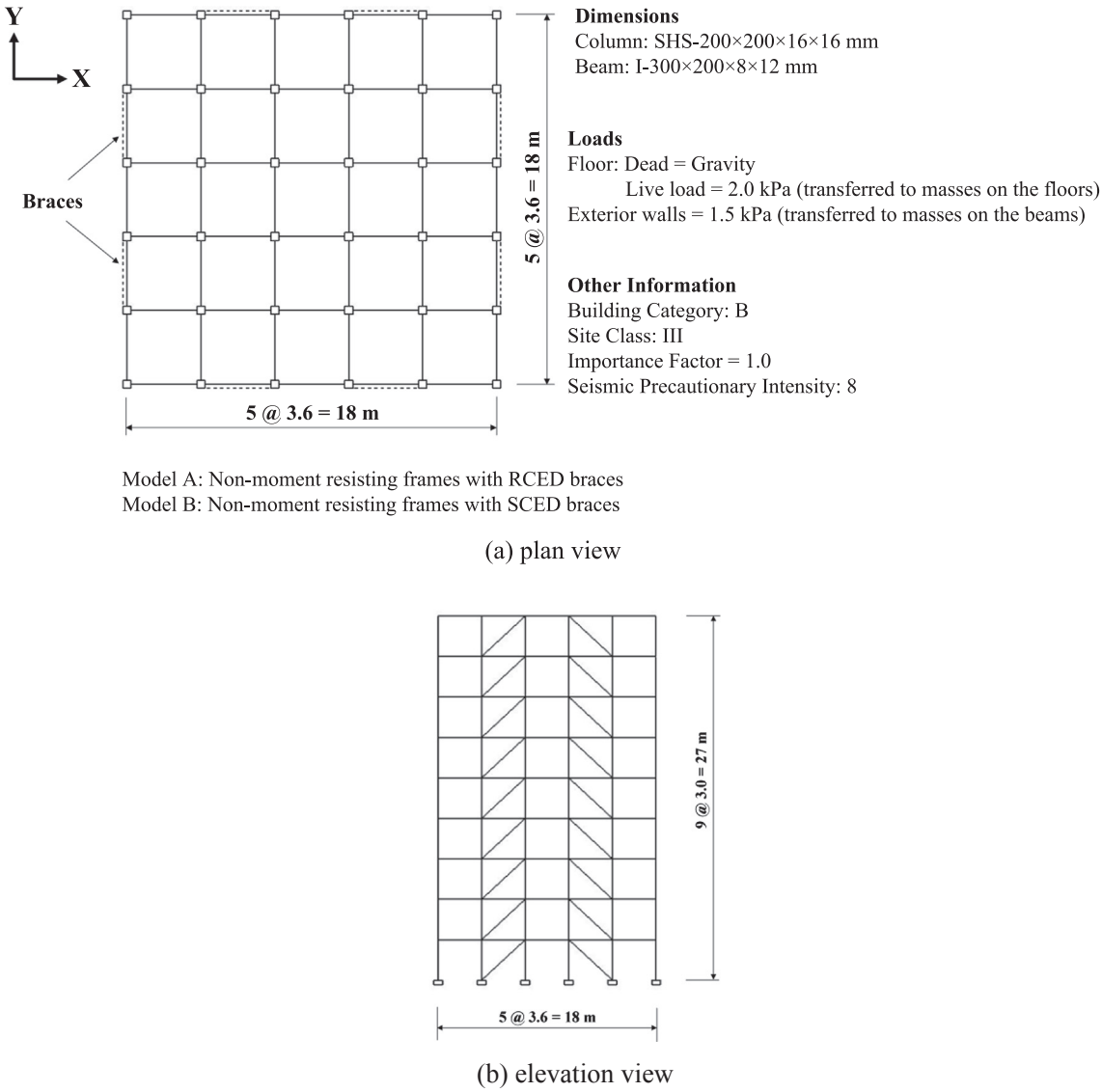

Fig. 7. Prototype of the multistory buildings.

4. Nonlinear time history analyses of multistory braced frames

4.1. FE models

Fig. 7 shows the prototype of the multistory buildings studied and some design parameters. Two symmetric buildings with five spans and nine stories were designed. The span was 3.6 m and the height of each story 3 m. Both models adopted nonmoment-resisting frames, while RCED and SCED braces were separately adopted. Table 3 describes the various FE models.

These two buildings were assumed to be located in Beijing, China. The building category was B, the site class III, the importance factor 1.0, and the seismic precautionary intensity 8. The cross section of the columns and beams were SHS-200 mm × 200 mm × 16 mm × 16 mm and I-300 mm × 200 mm × 8 mm × 12 mm, respectively. The live load on the floors was 2.0 kPa, which was transferred to the masses on the floors according to Chinese standard GB 50011 – 2010 [18]. Exterior walls were not established in the FE models; instead, they were replaced by the masses on the beams.

The FE models were developed using the ABAQUS software. B31 elements were adopted for the columns and beams, while T3D2 elements for the braces. S4R elements were used for the reinforcement concrete floors which were 200 mm in thickness. C40 concrete with a Young's modulus of 32.5 GPa, Poisson's ratio of 2.0, and density of 2.4 g/cm^3 was employed [19]. The "concrete damaged plasticity" was also defined. Two layers of Q345 steel rebars were embedded in the floors. The spacing of the rebars was 150 mm. Researchers have investigated prefabricated floors extensively [20,21] and many types of connections between floors and columns (or beams) have been proposed. The connection types will significantly affect the dynamic behavior of the entire structures. In the FE models, it was assumed that the floors had constraint effects on the beams but no effect on the columns.

In Model A, RCED braces with four steel tendons of diameter 21.5 mm in each group were utilized. Similar to the FE models in Section 3, the tendons were modeled using a steel member with a cross-sectional area of 746.4 mm. Two M20 high-strength bolts were employed in the frictional device. The coefficient of friction was set to 0.26, and a contact force of 620 kN was applied to each brace frame. The mechanical properties of the steel tendons were the same as those in Section 3.

In Model B, the SCED braces described in [22] were adopted, as shown in Fig. 8. As previously discussed, preloads are typically applied to the steel tendons to ensure the self-centering capacity of the braces. The tendons would always be subjected to a tension and hence would

Table 3
Description of the various FE models.

Model	Schematic	Cross section and length of braces	Contact force between A and C (kN)	Nonlinear elastic behavior between A and C	Note
A (Nonmoment-resisting frames with RCED braces)	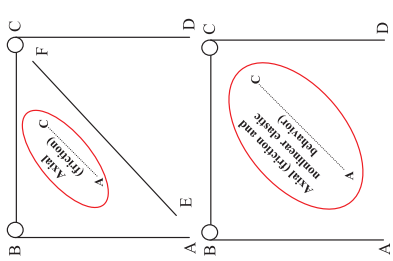	 Radius: 15.4 mm Cross-sectional area: 746.4 mm^2 length: 3800 mm	620	–	(a) The constraint effect of the floors on the beams was considered, but that on the columns were not accounted for. (b) The coefficient of friction of the RCED and SCED braces was 0.26. (c) The contact force equaled four times the pretension of a M20 high-strength bolt. (d) For Model B, The preload equaled 0.3 times the breaking forces of the tendons: 0.3 × 4 × 237.6 = 285.1 kN
B (Nonmoment-resisting frames with SCED braces)	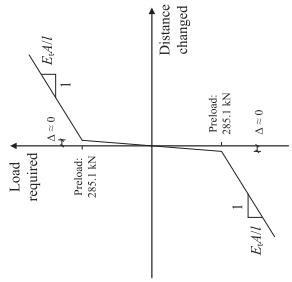	–	620		

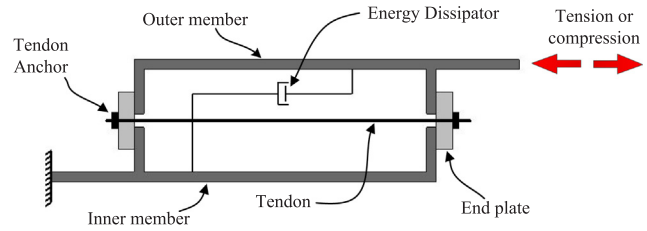

Fig. 8. SCED brace proposed by Christopoulos et al. [22].

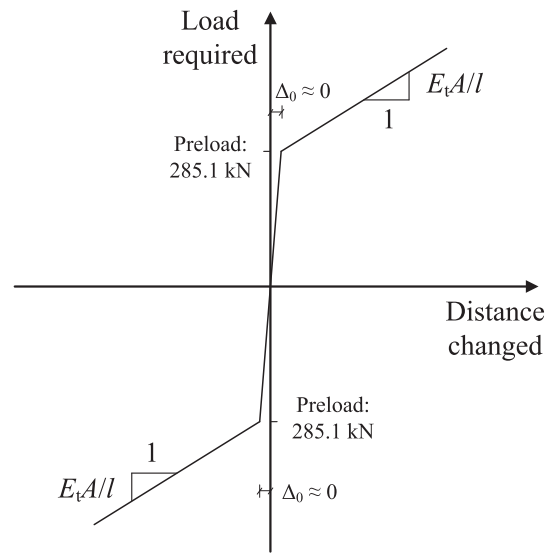

Fig. 9. Nonlinear elastic behavior of SCED braces (E_t, A, and l are the Young's modulus, cross-sectional area, and length of the steel tendons, respectively).

pull the brace back to its original location whether the brace was stretched or compressed. It is difficult to model the SCED brace by using only one or two steel members; meanwhile the nonlinear time history analysis will be time consuming if each part of the brace is modeled. Finally, we used the nonlinear elastic behavior defined between two points (Points A and C in Table 3) in the *Interaction* section in ABAQUS to realize the function of the SCED brace, as shown in Fig. 9. The figure illustrates that regardless of whether the distance between the two points increases or decreases, a load in the same direction is required. On the contrary, a load in the opposite direction generated by the nonlinear elastic behavior will be applied to the two points, which will pull them toward the original location. Theoretically, the distance Δ_0 should be equal to zero, whereas it will be inaccurate and an error will occur in ABAQUS if various values are defined for one point (the original point herein). Therefore, an extremely small value was assigned to Δ_0. As described in the Introduction, the effect of preload loss of the steel tendons on the self-centering behavior is reduced when the preload reaches 30–40% of the breaking force of the tendons. In this study, four steel tendons of diameter 21.5 mm (cross-sectional area of 186.6 mm^2) and a breaking force of 237.6 kN were employed. A preload that was 30% of the total breaking force was selected. Additionally, the coefficient of friction and contact force were the same as those of the RCED braces. It is noteworthy that the tendon forces of the SCED braces will be compared to those of the RCED braces in the next section. The tendon forces of the RCED braces can be easily obtained, because truss elements were adopted to model the RCED braces. However, the tendon forces of the SCED braces should be computed manually from the changed distance between A and C in the entire time history analysis and the nonlinear elastic behavior relationship.

Modal analyses of each FE model were firstly conducted. The results showed that Models A and B had the same first three vibration periods: 0.93, 0.93, and 0.53 s.

Table 4
Earthquake records selected for the nonlinear time history analyses.

Number	Year	Name	Recording station name	Recording station owner
1	1994	Northridge	Beverly Hills – Mulhol	USC
2	1979	Imperial Valley	El Centro Array # 11	USGS
3	1995	Kobe	Nishi-Akashi	CUE
4	1971	San Fernando	LA – Hollywood Stor	CDMG
5	1989	Loma Prieta	Capitola	CDMG
6	1999	Kocaeli, Turkey	Duzce	ERD

4.2. Comparative study

Six earthquake records obtained from the online PEER NGA database were selected for the nonlinear time history analyses, as shown in Table 4, which were all far-field records suggested by the FEMA P695 specification [23]. As per the Chinese code for seismic design [18], the peak earthquake acceleration for strong earthquakes (2% in a 50-year hazard level) under the seismic precautionary intensity of 8 was 400 cm^2/s in time history analyses, and the proportion of peak earthquake accelerations in the three directions (two horizontal and one vertical direction) was 1:0.85:0.65. The earthquake records were scaled according to this specification. Rayleigh damping with a damping ratio of 0.05 was adopted in the dynamic analysis.

Table 5 lists the results of the RCED and SCED models under the various earthquake records. Fig. 10 presents the results of these two models under the Northridge earthquake. As shown, both the RCED and SCED models experience the largest responses under the Kocaeli earthquake. The base shears of the SCED model are greater than those of the RCED model under the various earthquakes, except the Kocaeli earthquake.

In most cases, the SCED model dissipates more energy than the RCED model. Fig. 10(b) shows that the damping dissipation of the SCED model is significantly higher than that of the RCED model under the Northridge earthquake, contributing the difference in total energy dissipation. Fig. 10(b) also shows that the plasticity dissipations of these two models are fairly small, demonstrating that the steel frames of these models have not experienced large plastic deformations.

The total breaking force of the four steel tendons of diameter 21.5 mm was 950.4 kN. Table 5 shows that the maximum tendon force for the RCED model surpassed the total breaking force only under the Kocaeli earthquake, while the situation was worse for the SCED model. Fig. 10 suggests that the maximum ratio of tendon force to breaking force for the RCED model is 0.6 under the Northridge earthquake, while that for the SCED model is 1.21. The results demonstrate that some steel tendons of the SCED model at the second, third, fourth, and fifth floors will break under the Northridge earthquake action, which is highly dangerous. However, the steel tendons of the RCED braces are relatively safe under the Northridge earthquake and possess the capacity to carry larger loads.

Table 5 illustrates that the peak interstory drift primarily depends on the earthquake records. In some cases, the peak interstory drift of the RCED model is larger than that of the SCED model, while the trend is reversed in other cases. Fig. 10(d) shows the comparison of peak interstory drifts under the Northridge earthquake, in which Δ represents the interstory displacement and h_s the story height. It is clear that the drift on the fifth floor is the largest for the SCED model in this case, and the drift on the third floor is the largest for the RCED model.

The maximum residual interstory drift of the SCED model is always fairly small, owing to the preloads on the steel tendons. The greatest one is only 0.021% under the Kocaeli earthquake. The residual interstory drift of the RCED model is relatively large. However, the greatest one is 0.202%, which is still lower than 0.5%. It has been mentioned previously that the residual interstory drifts of the RCED model will decrease further if one loosens the high-strength bolts in the frictional device after an earthquake. It is noteworthy that the material of the steel tendons in the FE models is assumed to be elastic, and the break of steel tendons is not considered in the models.

4.3. Parametric study

In this section, a parametric study on the RCED model is presented. The effects of tendon diameter and pretension magnitude of high-strength bolts on the seismic performance of a multistory building with RCED braces were studied. It is noteworthy that the dynamic performance of a building is not only affected by the dynamic characteristics of the structure, but also by the earthquake acceleration record. As the building experienced the largest response under the Kocaeli earthquake, this earthquake record was selected in the parametric study.

4.3.1. Effect of tendon diameter

Four diameters were selected for the nonlinear time history analysis, i.e., 14, 17, 21.5, and 26 mm. The cross-sectional areas corresponding to the diameters are listed in Table 6. Similar to the models in Sections 3 and 4.1, these RCED models contain two groups of steel tendons and each group contains four tendons. Except the tendon diameter, the other parameters are the same as those of the RCED model in Section 4.1. The results are shown in Fig. 11, in which the letter D represents diameter and M20 the type of high-strength bolt.

Fig. 11(a) illustrates that the maximum base shear of the entire model increases with the tendon diameter. However, it is discovered from the comparison in Fig. 11(b) that the total energy dissipation increases with the tendon diameter. The plastic dissipations are still low and the frictional dissipations vary insignificantly. However, the variation of the damping dissipation is remarkable.

Fig. 11(c) shows the tendon forces. It is noteworthy that the breaking forces of steel tendons of diameters 17 and 21.5 mm listed in Table 1 are obtained from experimental tests [15], while the breaking forces of the steel tendons of diameters 14 and 26 mm are unknown. Therefore, the tendon forces instead of the ratios of the tendon force and breaking force are presented in Fig. 11(c). The results show that the tendon diameter will affect the maximum tendon force. With the

Table 5
Comparative results of the RCED and SCED models.

Earthquake records	RCED system (Maximum values)					SCED system (Maximum values)				
	Base shear (kN)	Total energy dissipation ($\times 10^6$ J)	Tendon force (kN)	Peak interstory drift	Residual interstory drift	Base shear (kN)	Total energy dissipation ($\times 10^6$ J)	Tendon force (kN)	Peak interstory drift	Residual interstory drift
Northridge	2341	2.138	589	1.25%	0.082%	3239	2.705	1246	1.55%	0.017%
Imperial Valley	1827	1.529	474	0.77%	0.091%	2352	1.716	710	0.65%	0.009%
Kobe	1770	1.105	355	0.73%	0.120%	2149	0.939	633	0.51%	0.007%
San Fernando	1512	1.703	285	0.63%	0.147%	2593	1.89	649	0.62%	0.006%
Loma Prieta	1585	1.295	276	0.62%	0.059%	2852	1.80	1022	0.97%	0.006%
Kocaeli, Turkey	3667	3.654	991	2.13%	0.202%	3633	4.61	1951	1.55%	0.021%

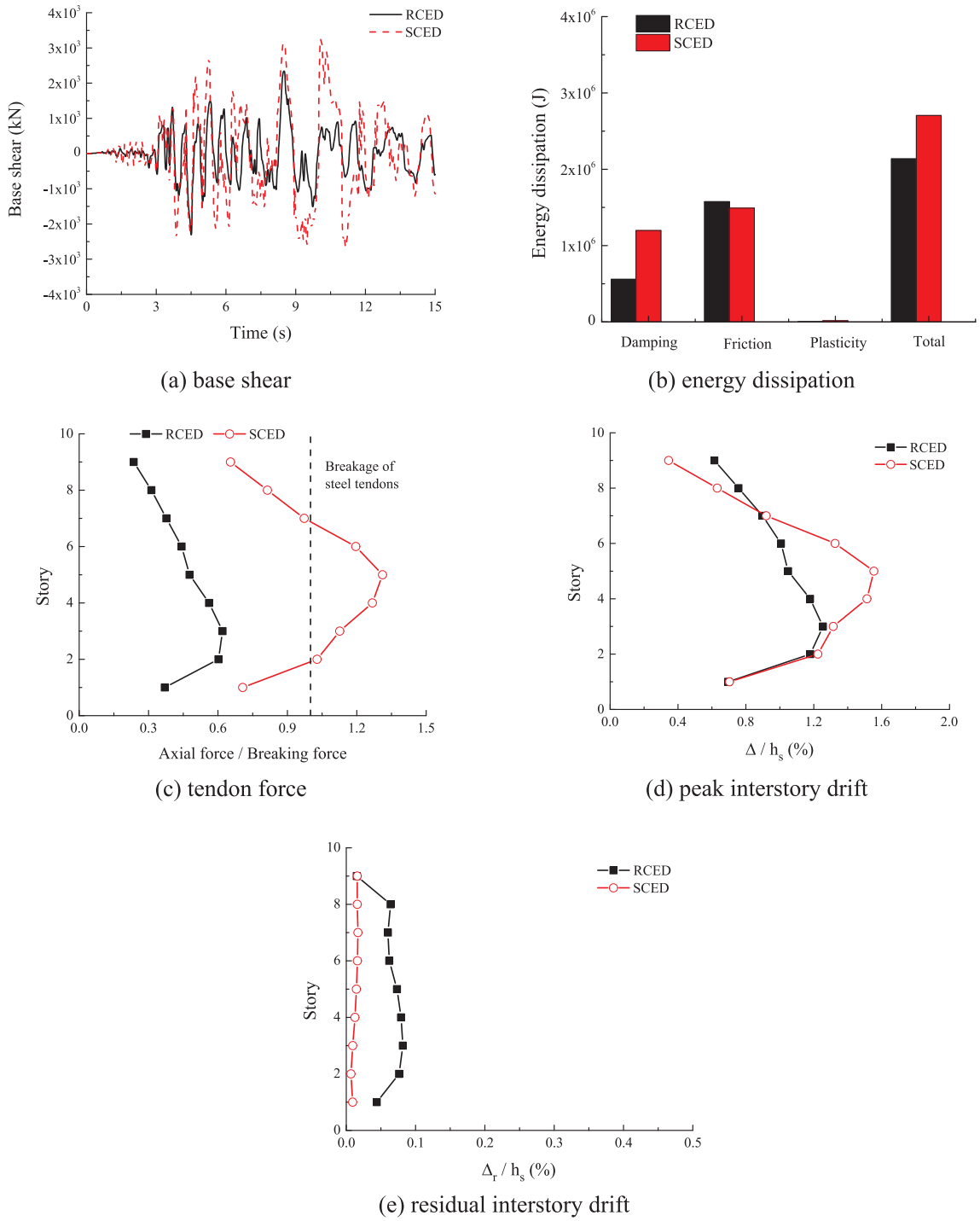

Fig. 10. Comparative results of the RCED and SCED models under the Northridge earthquake.

Table 6
Cross-sectional areas of the tendons for parametric study.

Diameter (mm)	14	17	21.5	26
Cross-sectional area (mm^2)	72.5	107.8	186.6	258.6

increase in the tendon diameter, the tendon force increases accordingly.

It is noted that the maximum peak interstory drift will decrease if the tendon diameter increases, which is advantageous for multistory buildings. Fig. 11(e) shows that the tendon diameter significantly affects the residual interstory drift under the Kocaeli earthquake. The shape of the curve and its maximum value vary markedly when the tendon diameter increases from 14 to 21.5 mm, which is caused by the combined effect of recentering and resistant forces. The resistant forces include the friction of the RCED braces and a force triggered by the plastic deformation of the building. The frictions of the RCED braces are the same in this section, while the plastic deformations (plasticity dissipations) are different. It is observed that even a small plastic deformation can significantly affect the residual drifts.

4.3.2. *Effect of pretension of high-strength bolts*

Four types of high-strength bolts were employed, i.e., M16, M20, M22, and M24. The pretensions corresponding to each type are listed in

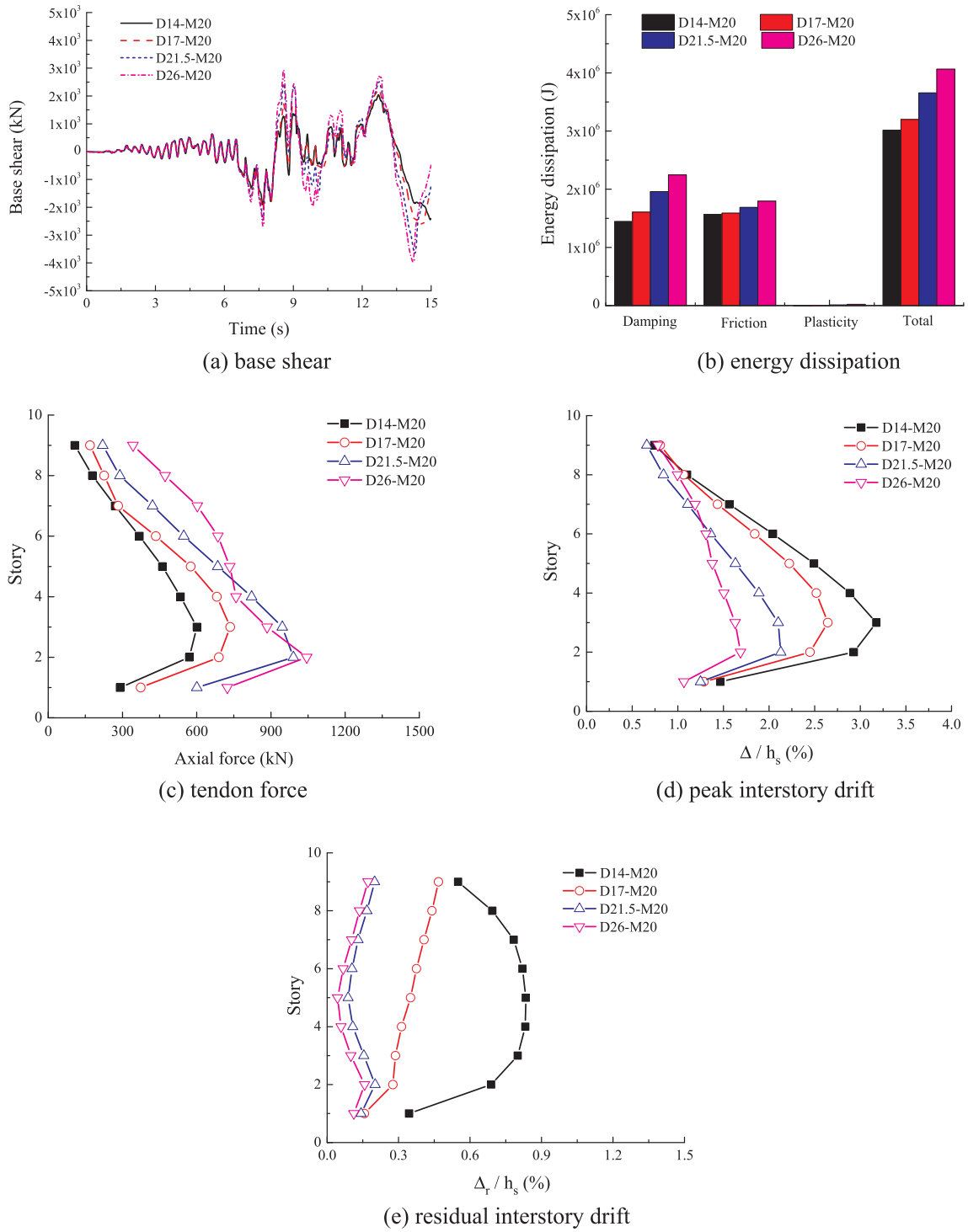

Fig. 11. Effect of tendon diameter on seismic performances of the RCED model (under the Kocaeli earthquake).

Table 7
Pretension of high-strength bolts.

Type	M16	M20	M22	M24
Pretension (kN) [24]	100	155	190	225

Table 7. For the models in this section, the tendon diameters are 21.5 mm. All the results under the Kocaeli earthquake are presented in Fig. 12.

It is observed that the pretension magnitude of the high-strength bolts has little effect on the base shear of the building under the Kocaeli earthquake. The total energy dissipation varies only slightly with the change in the high-strength bolts. The frictional dissipation increases with the pretension magnitude of the bolts, as expected. The plasticity dissipation is relatively high for the D21.5-M16 model compared with the other models, illustrating that the plastic deformation of this model is remarkable.

Fig. 12(c) shows that the larger the pretension of the bolts, the smaller is the maximum tendon force is. Fig. 12(d) shows that increasing the pretension of the bolts results in a decrease in the peak interstory drift. Fig. 12(e) suggests that the variation of the residual

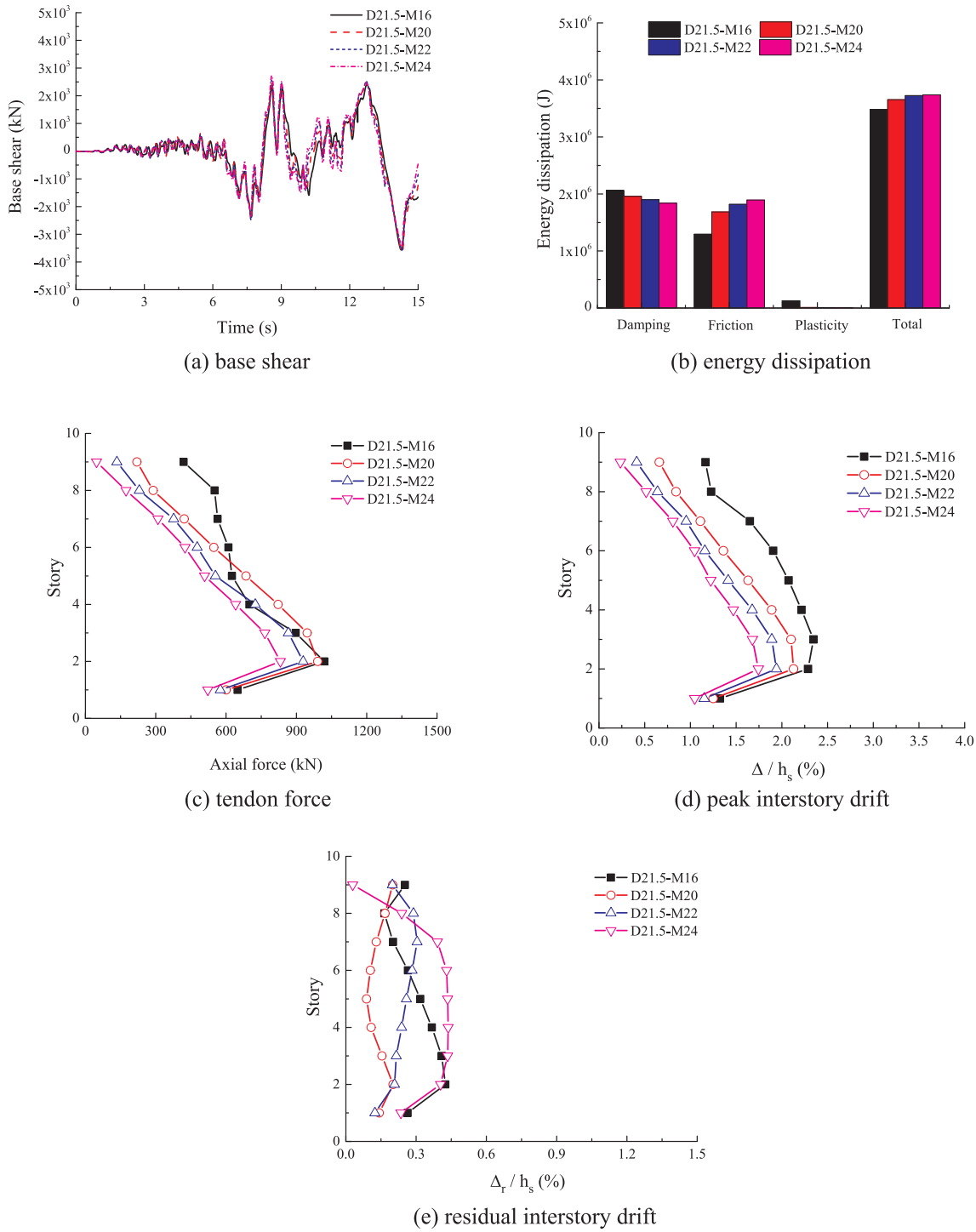

Fig. 12. Effect of pretension of high-strength bolts on the seismic performances of the RCED model (under the Kocaeli earthquake).

drift is irregular. As mentioned above, the resistance forces comprise the friction of the RCED brace, which is dominated by the pretension magnitude of the high-strength bolts and a force caused by plastic deformation. Therefore, the residual drift is not only determined by the pretension of the high-strength bolts. As the plasticity dissipation of the D21.5-M16 model is relatively high, the residual drifts of this model are large as well.

5. Conclusions

To reduce the effects of earthquake actions, many types of bracing systems have been developed. Based on previous research regarding bracing systems, Zhang and Ye [15] developed an RCED bracing system. They experimentally evaluated the hysteretic responses of steel frames with RCED braces. In this study, the seismic performance of steel frames with RCED braces was numerically investigated. The conclusions are as follows:

(1) For the one-bay steel braced frame, the hysteresis loops obtained from FE models agreed well with the experiment data. Therefore, the FE models developed in this study are suitable for predicting the experimental results.

(2) The comparative study indicates that the SCED model experienced a larger base shear and dissipated more energy than the RCED model in most cases. However, the maximum tendon force for the SCED model was significantly higher than that of the RCED model, demonstrating that the steel tendons in the SCED model were more prone to failure under earthquake actions. Owing to the preloads on the steel tendons, the SCED model experienced smaller residual drifts than the RCED model. However, the maximum residual drifts of the RCED model were small under the various earthquakes investigated in this study.
(3) Under the Kocaeli earthquake, the maximum base shear, total energy dissipation, and maximum tendon force of the RCED model increased whereas the peak interstory drift and residual drift decreased with the increase in the tendon diameter.
(4) The pretension magnitude of high-strength bolts had little effect on the base shear and total energy dissipation of the RCED model. However, increasing the pretension resulted in a decrease in tendon force and peak interstory drift. For the D215-M16 model, its plasticity dissipation was higher than those of the other models. Therefore, its maximum residual drift was high even though the friction resistance of the RCED brace was the smallest.

Declaration of Competing Interest

There is no conflict of interest.

Acknowledgement

The authors may wish to express their appreciation for financial support provided by the China Postdoctoral Science Foundation (Nos. 2019T120097 and 2018M630164). The experimental work described in this article was partially supported by the National Natural Science Foundation of China under Grant No. 51278010. However, the opinions and conclusions expressed in this article are solely those of the writers and do not necessarily reflect the views of the sponsors.

References

[1] Dai X, Zong L, Ding Y, et al. Experimental study on seismic behavior of a novel plug-in self-lock joint for modular steel construction. Eng Struct 2019;181:143–64.
[2] Deng E, Zong L, Ding Y, et al. Monotonic and cyclic response of bolted connections with welded cover plate for modular steel construction. Eng Struct 2018;167:407–19.
[3] Liu XC, He XN, Wang HX, et al. Bending-shear performance of column-to-column bolted-flange connections in prefabricated multi-high-rise steel structures. J Constr Steel Res 2018;145:28–48.
[4] Black CJ, Makris N, Aiken ID. Component testing, seismic evaluation and characterization of buckling-restrained braces. J Struct Eng – ASCE 2004;130(6):880–94.
[5] Chou CC, Chen SY. Subassemblage tests and finite element analyses of sandwiched buckling-restrained braces. Eng Struct 2010;32(8):2108–21.
[6] Tremblay R, Bolduc P, Neville R, et al. Seismic testing and performance of buckling-restrained bracing systems. Can J Civ Eng 2006;33(2):183–98.
[7] ANSI/AISC 341-16, Seismic Provisions for Structural Steel Buildings, American Institute of Steel Construction (AISC), Chicago, Illinois; 2016.
[8] Erochko J, Christopoulos C, Tremblay R. Design and testing of an enhanced-elongation telescoping self-centering energy-dissipative brace. J Struct Eng 2015;141(6):04014163.
[9] Desroches R, Taftali B, Ellingwood BR. Seismic performance assessment of steel frames with shape memory alloy connections. Part I Analysis and seismic demands. J Earthquake Eng 2010;14(4):471–86.
[10] Erochko J, Christopoulos C, Tremblay R. Design, testing, and detailed component modeling of a high-capacity self-centering energy-dissipative brace. J Struct Eng 2015;141(8):04014193.
[11] Erochko J, Christopoulos C, Tremblay R, et al. Shake table testing and numerical simulation of a self-centering energy dissipative braced frame. Earthquake Eng Struct Dyn 2013;42(11):1617–35.
[12] Tremblay R, Lacerte M, Christopoulos C. Seismic response of multistory buildings with self-centering energy dissipative steel braces. J Struct Eng – ASCE 2008;134(1):108–20.
[13] Chou CC, Chen JH. Development of floor slab for steel post-tensioned self-centering moment frames. J Constr Steel Res 2011;67(10):1621–35.
[14] Chou CC, Chung PT. Development of cross-anchored dual-core self-centering braces for seismic resistance. J Constr Steel Res 2014;101:19–32.
[15] Zhang A, Ye Q. Design and testing of prefabricated steel frame with an innovative re-centering energy dissipative brace. Eng Struct 2019;201:109791.
[16] Zhao J, Lin F, Wang Z. Effect of non-moment braced frame seismic deformations on buckling-restrained brace end connection behavior: theoretical analysis and subassemblage tests. Earthquake Eng Struct Dyn 2016;45(3):359–81.
[17] Bagheri S, Tabrizi NV. Effect of connection modeling on the seismic response of steel braced non-moment resisting frames. Struct Eng Mech 2018;68(5):591–601.
[18] GB 50011 – 2010. Code for seismic design of buildings. China Architecture & Building Press, Beijing, China; 2010.
[19] GB 50010 – 2010. Code for design of concrete structures. China Architecture & Building Press, Beijing, China; 2010 [in Chinese].
[20] Lukaszewska E, Johnsson H, Fragiacomo M. Performance of connections for prefabricated timber-concrete composite floors. Mater Struct 2008;41(9):1533–50.
[21] Lárusson LH, Fischer G, Jönsson J. Prefabricated floor panels composed of fiber reinforced concrete and a steel substructure. Eng Struct 2013;46:104–15.
[22] Christopoulos C, Tremblay R, Kim H-J, et al. Self-centering energy dissipative bracing system for the seismic resistance of structures: development and validation. J Struct Eng – ASCE 2008;134(1):96–107.
[23] Federal Emergency Management Agency. FEMA-P695 qualification of building seismic performance factors. Federal Emergency Management Agency: Washington, DC; 2009.
[24] JGJ 82-2011. Technical specification for high strength bolt connections of steel structures. China Architecture & Building Press, Beijing, China; 2011 [in Chinese].